Ignition Behavior of Hot Spheres Landing in Combustible Fuel Beds

Casey D. Zak, James L. Urban, and A. Carlos Fernandez-Pello
The University of California Berkeley
Berkeley, United States of America

1 Introduction

According to the National Fire Protection Association of the United States, wild land fires caused more than $600 million dollars in property damage and killed 65 civilians in the year 2011 [1]. These fires are also responsible for significant biomass consumption and a large source of combustion emissions to the atmosphere [2, 3]. Clearly, wildland and Wildland Urban Interface (WUI) fires have caused significant environmental and property damage, as well as the loss of life. Some of these fires allegedly begin when hot metallic particles land in combustible fuel beds, such as duff, litter or sawdust. These particles can be the result of powerline interactions, grinding or other industrial activities. Currently, the exact process by which this ignition occurs and the conditions necessary to initiate a spot fire are not well understood. Consequently, current wildland fire models lack capabilities for accurately predicting the initiation of spot fires [4,5]. A greater understanding of the ignition process and the conditions necessary for ignition could lead to improved predictive models and reduced losses due to fire.

There are only a few studies published on the ignition of fuel beds by hot metal particles [6–10]. The work presented here focuses on the ignition of powdered cellulose fuel beds by hot metallic spheres. The goal of this approach is to use a simplified laboratory case to understand the controlling parameters and underlying mechanisms at work in real world ignition scenarios. We utilized high-speed radial Schlieren video to investigate ignition behavior over a range of sphere diameters and temperatures. Schlieren techniques allowed us to observe pyrolyzate dynamics shortly before ignition, as well as more accurately identify the ignition time and location. In the following sections, we briefly describe our experimental method and then discuss the observed ignition statistics and behavior along with corresponding ignition times.

2 Experimental Description

In this investigation, stainless steel (alloy 302) spheres were heated using a tube furnace and dropped onto a fuel bed seated inside the test section of a bench-scale wind tunnel. The diameter and temperature of the spheres were varied between 2.38 mm and 15.88 mm and 625°C and 1100°C respectively. Stainless steel was chosen for the sphere material because of its commercial availability and the fact that

Correspondence to: czak@berkely.edu

it has a solidus temperature of 1400°C, well above the temperature range tested. This avoids the complication of phase change and the associated heat of fusion that may affect ignition behavior. Fuel beds were composed of powdered α-cellulose ($(C_6H_{10}O_5)_n$). Cellulose was chosen for its chemical homogeneity and the availability of property data. Furthermore, cellulose is the largest component of woody biomass, making it a reasonable surrogate for more complex fuels (such as sawdust or duff). According to data provided by the manufacturer (Sigma-Aldrich), the cellulose particle size distribution was approximately normal, with a mean of 0.19 mm and standard deviation of 0.36 mm. The settled volume of the fuel bed was held constant for all experiments. Here, the settled volume refers the minimum volume occupied by the fuel bed after vigorous vibration. Fuel bed bulk density varied between 239 and 341 kg/m^3, approximately the range stated by the manufacturer. The fuel beds were laboratory-conditioned; for each daily series of experiments, we measured the moisture content of the fuel and found it to have an average value of 6.28±0.41%.

The experimental apparatus is shown in figure 1a. The fuel bed is seated flush with the bottom of the wind tunnel. Laboratory air is flown through the wind tunnel section with a centerline velocity that decreases from 0.5 to 0.3 m/s across the length of the fuel bed. The tunnel top is opened to introduce the spheres and in most cases the top is kept open after the particle lands. Thus, the flow in the test section of the tunnel is a mixed free and forced flow. The relative humidity and temperature of the flow were measured daily and found to be 8.9±1.8% and 23.5±0.6°C respectively.

A linear guide holds a ceramic spoon approximately 140 mm above the fuel bed. This guide is collinear and concentric with a high-temperature tube furnace such that the spoon can easily be inserted and removed from the furnace. Viewing windows in the sides of the channel allow optical access for Schlieren video recording (see figure 1b). The Schlieren system utilizes a double pass configuration with a color bullseye (blue center, yellow and red rings) and a spherical mirror with a focal length of 1 m. Videos were recorded at 1200 frames per second (fps) using a digital camera.

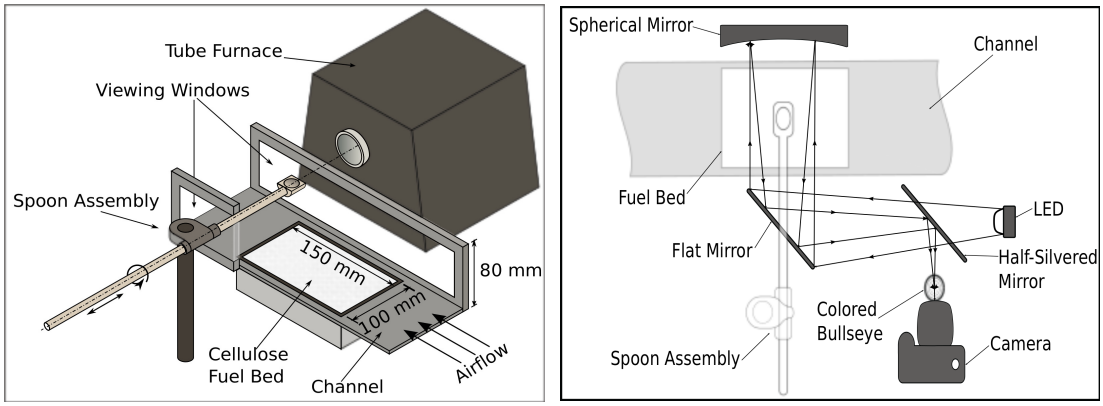

(a) (b)

Figure 1: Experimental Setup in (a) simplified isometric view with cutout, and (b) bird's eye view with optical setup

During each run, we placed a sphere in the ceramic spoon and inserted the spoon into the tube furnace. Once the sphere reached thermal equilibrium with the furnace, the spoon was rapidly removed from the furnace and rotated, dropping the sphere onto a virgin area of the fuel bed. For each set of test conditions, drop locations were varied and tests were performed on multiple beds to randomize contributing factors associated with the fuel bed and crossflow.

For the purposes of labeling each recorded event, we defined 'flaming ignition' as the appearance of a stable flame that persisted for more than 1 second after the sphere contacted the bed. Because the

scope of this work is restricted to flaming ignition, incipient smoldering ignition was recorded as a non-ignition event. Experiments focused on testing conditions near the flaming/non-flaming limit. Previous work by our lab has shown that relative to the parameters of interest, ignition behavior is stochastic in nature [9, 10]. Thus, at least five experiments were performed for each combination of diameter and temperature that we investigated.

3 Results

The ignition results are shown below in figure 2. Each circle denotes a combination of sphere diameter and temperature. The color of the circle indicates $\hat{p}$, the observed probability of ignition, calculated as

$$\hat{p} = \frac{\text{number of tests resulting in flaming ignition}}{\text{number of total tests}}. \tag{1}$$

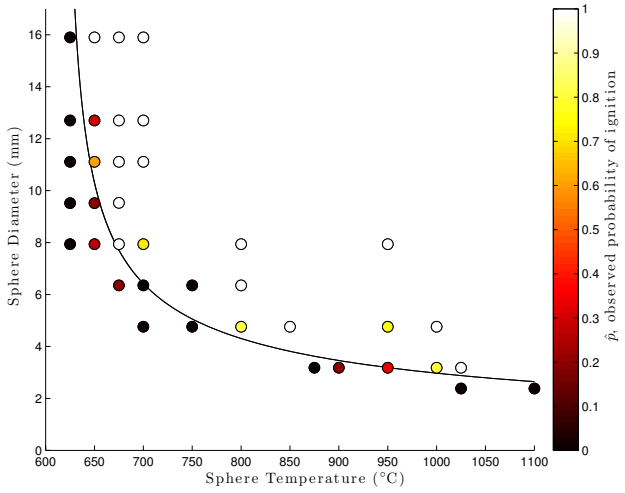

Figure 2: Ignition probability as a function of sphere diameter and temperature

We expect the ignition results to vary binomially since each test results in either ignition or no ignition. To more clearly represent the nature of the results, we performed a logistic regression on the data using the EUREQA *formalize* software package [11]. EUREQA uses machine-learning algorithms to assess the fit between a given data set and a large number of possible functional forms. The black trend line in figure 2 represents a 50% ignition probability according to this regression. This line is given by the equation

$$971.218 d_s^2 + 3280.93 d_s^2 T_s^2 - 23290.7 = 0, \tag{2}$$

where d_s and T_s are the diameter and temperature of the sphere, respectively. Further testing is required before this type of fitting can yield any physical insight, but the trend line is useful for visualizing ignition behavior. Assuming the line represents the best fit of the data, all diameter/temperature pairs located to the right of the line have a greater probability of igniting than not igniting; the opposite is true for those pairs to the left of the line. The data agrees qualitatively with previous studies in that smaller spheres require higher temperatures to cause ignition [6, 9, 10]. It also indicates asymptotic behavior at low temperatures and small diameters. No spheres caused ignition at 625°C, despite many tests being

performed at that temperature. Similarly, spheres 2.38 mm in diameter were never found to ignite at the temperatures studied. Further work is required to confirm that spheres of this size do not ignite at temperatures greater than 1100°C.

Following completion of the experiments, high-speed video of each of the events was analyzed. A sequence of still frames from two ignition events are shown in figures 3a and 3b. Figure 3a depicts ignition involving a 15.9 mm sphere at 650°C, while figure 3b depicts a 3.18 mm ball heated to 950°C. The small red circle that appears near the upper lefthand corner of all frames is an artifact of the Schlieren imaging technique and is not involved in the ignition process.

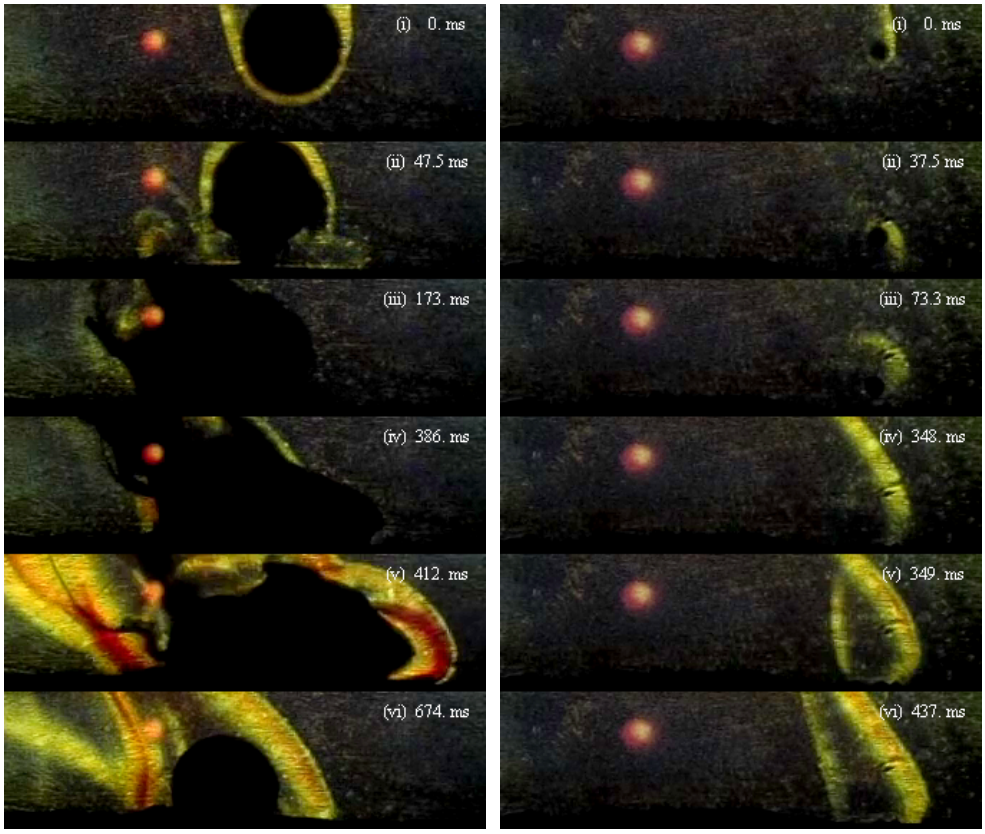

(a) (b)

Figure 3: Still frames of ignition sequence for spheres with (a) $d_s = 15.9$ mm, $T_s = 650$°C and (b) $d_s = 3.18$ mm, $T_s = 950$°C

A general sequence of events is common to all recorded tests. First, the sphere, followed by its Schlieren contrail, is seen impacting the fuel bed (frames **i**, figure 3). The majority of spheres then bounce and may or may not spin (frames **ii**, figure 3). Upon impact, a Schlieren contour expands away from the sphere, indicating the expansion or growth of a hot gas volume. Initially, this may be hot air being pushed out of the way by the impinging sphere, but a continued presence indicates the production of gaseous pyrolyzate generated as the sphere heats the surface of the fuel bed or some sort of pre-ignition reaction zone. Cellulose particles are sometimes visibly lofted by the impact of the sphere. The current resolution of the videos (0.22 mm) means that smaller unobservable particles may also be lofted, and it is not clear whether combustion initiates in a dust cloud or a gaseous mixture or a combination of both. Further study is needed to understand the composition of the material within this initial Schlieren contour.

In the cases of non-ignition, a dark plume is observed emanating from the sphere and surrounding fuel

bed at some time after the initial impact. A dark appearance in a Schlieren image means an object is opaque, suggesting either cellulose particles lofted by the ball's impact or heavier products of pyrolysis. These plumes do not appear to behave like lofted particles, but it may be comprised of many very small particles. Assuming the cloud is at least partially fluid in nature, it seems likely that the opacity is due to a combination of solid and condensed pyrolysis products.

When ignition does occur, it is clearly observed as a rapid expansion of the existing hot gas contour, or as a second contour that nucleates within the first (frames **v**, figure 3). After the flame front is initiated, it grows in size and eventually anchors to the fuel bed, becoming a diffusion flame. The rapid expansion of ignition is clearly illustrated in the differences between frames **iv** and **v** in figure 3b, which were taken less than 1 ms apart. The intensity of the Schlieren perturbation also increases, to the point that red is observed (frames **iv**-**vi**, figure 3a). When a second contour is observed, its location can vary greatly; ignition occurred on both the bottom and top surfaces of spheres during bouncing, as well as up to 10 mm away from the sphere within the hot gas volume. This latter finding is interesting in that it shows that the combustion reaction does not necessarily initiate at the surface of the hot sphere. Additionally, the video footage indicates that ignition distance from the sphere increases with increasing temperature.

We recorded ignition times for the majority of events, and the average times for many diameter and temperature combinations are displayed in figure 4. Here, ignition time is defined as the time between when a sphere first contacts the fuel bed and the first sign of ignition.

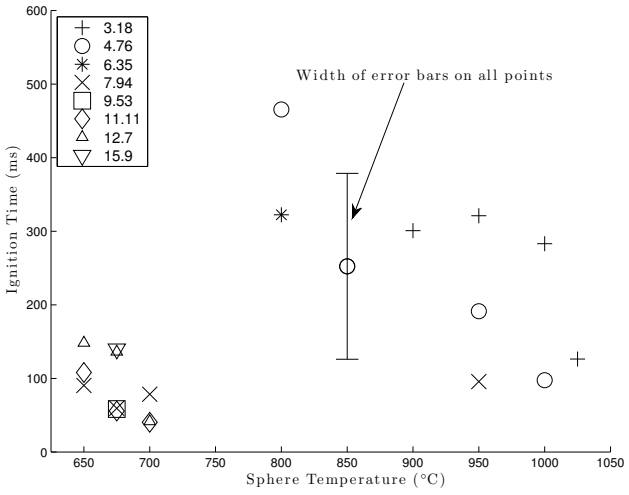

Figure 4: Ignition times

As indicated by the error bar in the plot, there is a great amount of variability in the recorded ignition times. The data suggest two interesting trends. First, it appears that ignition times tend to decrease with increasing temperature for a given sphere diameter. Second, when comparing ignition times near a sphere's ignition limit, smaller spheres ($d_s <= 6.35$ mm) seem to generally have longer ignition times. This trend may be affected by the fact that smaller spheres tended to bounce higher and spend more time in the air away from the fuel bed. Overall, it was noted that the trajectory the ball could very strongly change the ignition time. However, smaller spheres may also transfer energy to the fuel bed in a different way, and this may affect the ignition process.

In addition to the differences between large and small spheres suggested by figure 4, other qualitative differences are apparent in the high-speed videos. The larger balls had a greater propensity to have clumps of cellulose attached to them after impact and produce dark pyrolysate plumes, even for cases

where ignition occurred (see figure 3a, frames **iii**-**v**). In the case of the smaller diameter balls, wisps of dark pyrolyzate were only occasionally observed and generally the pyrolyzate was only indicated by the Schlieren contour. Brief combustion events were also noticed for several small spheres near their apex, as discussed in previous work by our laboratory. These 'flashes' did not result in a stable flame.

4 Conclusions

Ignition tests have been performed over a range of sphere temperatures and diameters, and the boundaries of ignition have been determined for steel spheres of varied diameters. Video and high-speed schlieren imaging were used to observe and describe the ignition process. Many aspects of the observed behavior are the result of the chosen fuel bed and as a result, the applicability of this work may be restricted to powdered fuels. Ignition propensity appears to behave asymptotically at small diameters and low temperatures (particularly the latter). The differences in qualitative behavior and average ignition times between these two asymptotic regions suggest that there may be different dominant controlling mechanisms in each of the two limits. Future work in this area will be focused on identifying these mechanisms and refining the ignition propensity and ignition time data presented above.

References

[1] M. Karter, "Fire loss in the united states during 2011," September 2012.

[2] G. Rein, S. Cohen, and A. Simeoni, "Carbon emissions from smouldering peat in shallow and strong fronts," *Proc. Combust. Inst.*, vol. 32, pp. 2489–2496, 2009.

[3] S. Page, F. Siegert, J. Rieley, H. Boehm, A. Jaya, and S. Limin, "The amount of carbon released from peat and forest fires in indonesia during 1997," *Nature*, vol. 420, pp. 61–65, 2022.

[4] M. Finney, "Farsite: Fire area simulator-model development and evaluation, research paper rmrs -rp4," U.S. Department of Agriculture, Forest Service, Rocky Mountain Research Station, Tech. Rep., 1998.

[5] R. Linn, J. Resiner, J. Colman, and J. Winterkamp, "Studying wildfire behavior using firetec," *Intl. Journal of Wildland Fire*, vol. 11, pp. 233–246, 2002.

[6] G. Rowntree and A. Stokes, "Fire ignition by aluminum particles of controlled size," *Journal of Elec. and Electronics Engr., Australia*, vol. 14, pp. 117–123, 1994.

[7] C. Rallis and B. Mangaya, "Ignition of veld grass by hot aluminium particles ejected from clashing overhead transmission lines," *Fire Tech.*, vol. 38, pp. 81–92, 2002.

[8] T. Tanaka, "On the flammability of combustible materials by welding splatter," *Reports of the Natl. Research Inst. of Police Sci.*, vol. 30, pp. 151–158, 1977.

[9] R. Hadden, S. Scott, C. Lautenberger, and A. C. Fernandez-Pello, "Ignition of combustible fuel beds by hot particles: An experimental and theoretical study," *Fire Tech,*, vol. 47, pp. 341–355, 2011.

[10] C. Zak, "Powdered fuel bed ignition by heated particles: An experimental and phenomenological study," Master's thesis, University of California Berkeley, 2012.

[11] M. Schmidt and H. Lipson, "Distilling free-form natural laws from experimental data," *Science*, vol. 324, pp. 81–85, 2009.